Artesunate promotes cervical cancer cell apoptosis by regulating Bcl2 family molecules and reducing the mitochondrial membrane potential

QIANYING ZHANG[1], XING LI[2], CAIYI HE[2], RONGMIAO ZHOU[3], JING WANG[2] and LIANG LIU[2]

[1]Department of Gynaecological Oncology, The Fourth Hospital of Hebei Medical University; Departments of [2]Flow Cytometry and [3]Molecular Biology, Tumour Institute, The Fourth Hospital of Hebei Medical University, Shijiazhuang, Hebei 050011, P.R. China

Received October 11, 2023; Accepted April 3, 2024

DOI: 10.3892/ol.2024.14447

Abstract. Artesunate (ART), an antimalarial drug, has a broad spectrum of antitumour effects in cancer types such as esophageal and gastric cancer. However, evidence demonstrating the role of ART in cervical cancer cells is limited. In the present study, the inhibitory effect of ART on the growth of cervical cancer cells through the modulation of the cell cycle and apoptosis was investigated. The growth-inhibitory effect of ART on a cervical cancer cell line (SiHa) was detected using a Cell Counting Kit-8 assay after treatment with ART for 24 h, after which the half-maximal inhibitory concentration (IC_{50}) was calculated. Using flow cytometry assays, apoptosis, the cell cycle, the levels of reactive oxygen species (ROS) and calcium (Ca^{2+}) ions, as well as the mitochondrial membrane potential were evaluated in SiHa cells following treatment with ART for 24 and 48 h. The mRNA expression levels of Bcl2, Bcl-xl, (myeloid cell leukaemia 1) Mcl-1, Bcl2-like protein 11 (BIM), (Bcl2-related ovarian killer protein) Bok, Bax and (Bcl2 homologous antagonist/killer) Bak in SiHa cells were detected using reverse transcription-quantitative PCR. ART inhibited the growth of SiHa cells in a dose-dependent manner. The IC_{50} of ART in SiHa cells was 26.32 μg/ml. According to the IC_{50} value, 15, 30 and 100 μg/ml ART were selected for further experiments, and normal saline (0 μg/ml ART) was used as the control group. The results indicated that treatment with 15, 30 and 100 μg/ml ART for 24 and 48 h induced apoptosis, increased the levels of ROS, the levels of Ca^{2+} and the mRNA expression levels of BIM, Bok, Bax and Bak, but decreased the cell proliferation indices, the mitochondrial membrane potential and the mRNA expression levels of Bcl2, Bcl-xl and Mcl-1 in a dose- and time-dependent manner. In conclusion, ART inhibited the growth of SiHa cells and induced apoptosis via a mechanism associated with the regulation of Bcl2 family member expression, which was associated with the increase of the levels of ROS and Ca^{2+} and the reduction of the mitochondrial membrane potential.

Introduction

Cervical cancer is a common malignant tumour in women worldwide that is associated with high morbidity and mortality, threatening the life and health of female patients. According to Global Cancer Statistics 2020 (GLOBOCAN 2020 data) (1), the incidence and mortality of cervical cancer rank fourth among all malignant tumours in women worldwide, accounting for ~6.5 and 7.7%, respectively. The China Cancer Registry data showed that the mortality-to-incidence ratio was 0.30 in 2014. In 2014, ~102,000 new cases of cervical cancer were estimated to have occurred in China, with a crude incidence rate of 15.30/100,000 (2). Currently, the conventional treatment methods for cervical cancer include surgery, radiotherapy and chemotherapy (3,4), but the toxic side effects of chemotherapy drugs and the occurrence of drug resistance affect the treatment efficacy (5). Therefore, it is important to identify low-toxicity and high-efficiency anticancer drugs.

Chinese herbal medicine has a history in the treatment of cancer, and its low toxicity and side effects provide it with unique characteristics in the treatment of cancer. Artesunate (ART), derived from artemisinin, is an antimalarial drug, used for severe and drug-resistant malaria (6-8). ART has antioxidant, immunomodulatory and antitumour effects in addition to its antimalarial effects (9-11). The antitumour effects of ART have been previously studied and the results showed that ART has growth-inhibitory effects on a variety of tumour cells, with low toxicity and side effects (12-15). The study by Våtsveen *et al* (16) demonstrated that ART has potent apoptosis-inducing effects on a broad range of B-cell lymphoma cell lines both *in vitro* and *in vivo*. Furthermore,

Correspondence to: Professor Liang Liu, Department of Flow Cytometry, Tumour Institute, The Fourth Hospital of Hebei Medical University, 12 Jiankang Road, Shijiazhuang, Hebei 050011, P.R. China
E-mail: lianglhebmu@hebmu.edu.cn

Abbreviations: ART, artesunate; IC_{50}, half-maximal inhibitory concentration

Key words: cervical cancer, ART, mitochondrial membrane potential, reactive oxygen species, calcium ions, Bcl2 family, cell apoptosis

the study by Yin *et al* (17) indicated that ART could be an effective antitumour agent through modulating the oestrogen receptor (ER)-α-mediated liver kinase B1/AMP-activated protein kinase/mTOR pathway in a heart- and neural crest derivatives-expressed protein 2-dependent manner, and that ART is an effective therapeutic agent for ER-α-positive endometrial cancer. The study by Mancuso *et al* (18) reported that ART inhibits the growth of leukaemia, multiple myeloma and lymphoma cells by inducing cell apoptosis, autophagy and ferroptosis. Additionally, other studies indicated that ART inhibits the growth of oesophageal cancer and gastric cancer cells by inducing apoptosis (19,20). However, there are only a small number of reports on the molecular mechanism by which ART inhibits cervical cancer, such as the study by Saeed *et al* (21).

Apoptosis is a type of cell death, in which the orderly and autonomous death of cells controlled by genes can eliminate abnormal cells in the body. This serves an important role in maintaining the stability of the internal environment. Apoptosis is an active form of cell death controlled by multiple genes, including those of the Bcl2 and caspase families, and is regulated by multiple pathways, including the membrane receptor pathway and the mitochondrial pathway. The mitochondria-mediated apoptosis pathway is associated with the antitumour effect of drugs, such as epigallocatechin-3-gallate (22). Mitochondria are unique and important organelles and are the 'power factories' of the cell (23). Changes in mitochondrial function are associated with apoptosis and participate in the process of apoptosis by releasing proapoptotic factors, increasing the generation of reactive oxygen species (ROS), and increasing intracellular calcium (Ca^{2+}) ion levels (24-26). There are numerous members of the Bcl2 family, including Bcl2, Bcl-xl, (myeloid cell leukaemia 1) Mcl-1, Bcl2-like protein 11 (BIM), (Bcl2-related ovarian killer protein) Bok, Bax and (Bcl2 homologous antagonist/killer) Bak. These proteins have either antiapoptotic or proapoptotic effects. Most members of the Bcl2 family have two structural homology regions through which different members can form heterodimers, and Bcl2 members are functional or functionally regulated through dimerization. Bcl2 can localize to mitochondria, stabilize the mitochondrial membrane potential, prevent apoptosis and protect cells (27). Dysfunction of the expression of Bcl2 family members can cause dysregulation of apoptosis and lead to the occurrence of diseases, including cancer and autoimmune diseases (27). Tumour cells have the ability to avoid apoptosis and survive, thus, apoptotic disorders can lead to malignant tumours (28).

In the present study, the anticancer effects of ART *in vitro* and the associated molecular mechanisms of a low-toxicity and high-efficiency dose of ART for the clinical treatment of cervical cancer were investigated.

Materials and methods

Cancer cell line and culture. The SiHa cell line (cat. no. CL-0210) was obtained from Procell Life Science & Technology Co., Ltd., and was cultured in minimum essential medium (MEM) supplemented with 10% FBS and 1% penicillin and streptomycin (cat. no. CM-0210; Procell Life Science & Technology Co., Ltd.). The cells were maintained in an incubator at 37˚C with 5% CO_2.

Chemicals and reagents. ART was purchased from Guilin Pharmaceutical (Shanghai) Co., Ltd. An annexin V-phycoerythrin (PE)/7-aminoactinomycin D (7-AAD) kit (cat. no. 559763) and propidium iodide were purchased from BD Biosciences. The primers used in the present study were purchased from Sangon Biotech Co., Ltd.

Cytotoxicity assay. The cells were seeded in 96-well plates at a density of $1x10^4$ cells/well. Once the cells were attached, serially diluted ART solution was added at a final concentration of 0.5 1, 5, 10, 50, 100, 400 or 800 μg/ml in a final volume of 200 μl/well. Normal saline (NS) was used for the control group. After drug treatment for 24 h at 37˚C, the medium was replaced with an equivalent volume of fresh MEM containing 20 μl Cell Counting Kit-8 (CCK-8; Wuhan Boster Biological Technology, Ltd.), followed by incubation for an additional 2 h. The cytotoxic effects of ART were determined by measuring the optical density at 450 nm using a microplate reader. The growth inhibition rate was calculated as follows: [(1-absorbance of the ART treated group)/absorbance of the control group] x100.

ART intervention experiments. SiHa cells were seeded in 6-well plates at a density of $1x10^5$ cells/well. Once the cells reached 80-85% confluence, ART was added to each well at concentrations of 15, 30 and 100 μg/ml, and NS was added to the control group. ART concentrations of 15, 30 and 100 μg/ml were selected that were close to the half-maximal inhibitory concentration (IC_{50}) value of ART. After ART treatment for 24 and 48 h at 37˚C, SiHa cells were collected using centrifugation (200 x g, 25˚C, 5 min). The cell concentration was adjusted to $1x10^6$/ml. Each experiment was repeated three times. SiHa cells treated with NS or 15, 30, or 100 μg/ml ART were referred to as the control and 15, 30 or 100 μg/ml ART groups, respectively.

Assessment of cell apoptosis using flow cytometry (FCM). A SiHa cell suspension (1 ml containing $1x10^6$ cells/ml) was collected, washed once with cold PBS (4˚C), and resuspended in 100 μl 1X binding buffer. Subsequently, 5 μl annexin V-PE was added, and the mixture was placed on ice for 15 min in the dark. Next, 390 μl 1X binding buffer and 5 μl 7-AAD were added, and the mixture was incubated for 15 min in the dark at 37˚C. Cell apoptosis was measured using a FC500 flow cytometer (Beckman Coulter, Inc.). The EXPO32 ADC software version 1.2 (Beckman Coulter, Inc.) was used to analyse the fluorescence data and evaluate the apoptosis rate.

Assessment of cell cycle distribution using FCM. SiHa cell suspension (1 ml) was fixed with 70% ethanol at 4˚C for 24 h. Subsequently, the cells were washed once with cold PBS (4˚C), and 1 ml propidium iodide (containing RNAse A) was added before incubation at 4˚C in the dark for 30 min. The cells were then measured using a FC500 flow cytometer, and the cell cycle data were analysed using MultiCycle AV software version 275 (Phoenix Flow Systems, Inc.). The proliferation index (PI) was calculated using the following formula:

PI=(S + G_2/M)/($G_{0/1}$ + S + G_2/M) x100%. The PI represents the state of cell proliferation (29).

Flow cytometric analysis of the generation of ROS in SiHa cells after ART treatment. SiHa cells were washed with cold PBS (4˚C), and stained with 1 ml dichlorodihydrofluorescein diacetate (5 μg/ml; Cayman Chemical Company) for 30 min in the dark at 37˚C. The stained cells were then washed once with cold PBS (4˚C), resuspended in 1 ml PBS, and analysed using a FC500 flow cytometer. Fluorescence data were analysed using EXPO32 ADC software version 1.2.

Analysis of Ca^{2+} levels in SiHa cells after ART treatment using FCM. SiHa cells were washed with cold PBS (4˚C), and stained with 1 ml Fluo-3 AM (1 μM; Beyotime Institute of Biotechnology) for 30 min in the dark at 37˚C. The stained cells were then washed once with cold PBS (4˚C), resuspended in 1 ml PBS, and analysed using a FC500 flow cytometer. Fluorescence data were analysed using EXPO32 ADC software version 1.2.

Flow cytometric analysis of the mitochondrial membrane potential of SiHa cells after ART treatment. SiHa cells were washed with cold PBS (4˚C), and stained with 0.5 ml JC-1 reagent (Beyotime Institute of Biotechnology) for 20 min in the dark at 37˚C. The stained cells were then washed twice with 1X JC-1 staining buffer, resuspended in 1 ml 1X JC-1 staining buffer, and analysed using a FC500 flow cytometer. Fluorescence data were analysed using EXPO32 ADC software version 1.2 and presented as the ratio of JC-1 aggregates/JC-1 monomers.

Evaluation of mRNA expression levels using reverse transcription-quantitative PCR (RT-qPCR). SiHa cells were collected using centrifugation (200 x g, 25˚C, 5 min) and washed once with PBS. Total RNA was extracted from the cells using 1 ml RNA isolater (Vazyme Biotech Co., Ltd.). As the template for PCR, cDNA was synthesized using the HiScript II First Strand cDNA Synthesis kit (Vazyme Biotech Co., Ltd.) according to the manufacturer's protocol. Based on the manufacturer's protocol for the qPCR SYBR-Green Master Mix kit (Vazyme Biotech Co., Ltd.), qPCR was performed. The primer sequences used were: Bcl2 forward, 5'-ATCGCCCTGTGGATGACTGAGT-3' and reverse, 5'-GCCAGGAGAAATCAAACAGAGGC-3'; Bcl-xl forward, 5'-GCCACTTACCTGAATGACCACC-3' and reverse, 5'-AACCAGCGGTTGAAGCGTTCCT-3'; BIM forward, 5'-CAAGAGTTGCGGCGTATTGGAG-3' and reverse, 5'-ACACCAGGCGGACAATGTAACG-3'; Mcl-1 forward, 5'-CCAAGAAAGCTGCATCGAACCAT-3' and reverse, 5'-CAGCACATTCCTGATGCCACCT-3'; Bax forward, 5'-TCAGGATGCGTCCACCAAGAAG-3' and reverse, 5'-TGTGTCCACGGCGGCAATCATC-3'; Bak forward, 5'-TTACCGCCATCAGCAGGAACAG-3' and reverse, 5'-GGAACTCTGAGTCATAGCGTCG-3'; Bok forward, 5'-ACGCCTGGCTGAGGTGTGCG-3' and reverse, 5'-AGGAACGCATCGGTCACCACAG-3'; and GAPDH forward, 5'-GTCTCCTCTGACTTCAACAGCG-3' and reverse, 5'-ACCACCCTGTTGCTGTAGCCAA-3'. The internal reference used was human GAPDH. The thermocycling procedure used was as follows: Initial denaturation at 95˚C for 5 min; followed by 40 cycles of 95˚C for 10 sec and 60˚C for 30 sec. Dissociation was performed at 95˚C for 15 sec, 60˚C for 1 min and 95˚C for 15 sec. For each sample, each experiment was repeated three times. The relative mRNA expression levels of Bcl2, Bcl-xl, Mcl-1, BIM, Bok, Bak and Bax were calculated using the $2^{-\Delta\Delta Cq}$ method (30).

Statistical analysis. All the data are presented as the mean ± SD (n=3). Two-way ANOVA were performed to compare multiple groups, followed by the Bonferroni post hoc test. The data were analysed using SPSS software (version 21; IBM Corp.). P<0.05 was considered to indicate a statistically significant difference.

Results

Inhibitory effect of ART on SiHa cells. As shown in Fig. 1A, SiHa cell survival decreased in a dose-dependent manner after treatment with different concentrations of ART ranging from 0.5-800 μg/ml for 24 h. After treatment with ART for 24 h, the IC_{50} was 26.32 μg/ml. Based on the IC_{50} value, three concentrations of ART (15, 30 and 100 μg/ml) were selected for the subsequent experiments.

In addition, the proliferation indices of SiHa cells were notably reduced in the ART-treated groups compared with that in the control group in a dose- and time-dependent manner. Furthermore, the proportion of cells in the $G_{0/1}$ phase was notably increased in the ART-treated groups compared with that in the control group in a dose- and time-dependent manner (Fig. 1B and C).

ART induces SiHa cell apoptosis. After exposure to various concentrations of ART (15, 30 or 100 μg/ml) for 24 or 48 h, with 0 μg/ml ART used as the control, SiHa cells exhibited a dose- and time-dependent apoptosis as demonstrated using Annexin V-PE/7-AAD staining and FCM (Fig. 2A).

The total apoptosis rate of SiHa cells, including the early apoptosis rate and late apoptosis rate, was increased by 15, 30 or 100 μg/ml ART in a dose- and time-dependent manner (Fig. 2B). The total apoptosis rates of SiHa cells in the 15, 30 and 100 μg/ml ART groups were significantly increased compared with that in the control group (P<0.01). Furthermore, the total apoptosis rate of SiHa cells in the 100 μg/ml ART group was significantly increased compared with that in the 15 and 30 μg/ml ART groups (P<0.01). In addition, with the increasing treatment duration and dose of ART, the late apoptosis rate increased compared with that of the control group (P<0.05; Fig. 2C). The early apoptosis rates of SiHa cells in the 15, 30 and 100 μg/ml ART groups were significantly increased compared with that in the control group (P<0.01; Fig. 2D). The percentages of live cells in the 15, 30 and 100 μg/ml ART groups were significantly decreased compared with that in the control group (P<0.01; Fig. 2E).

ART modulates ROS production, Ca^{2+} levels and the mitochondrial membrane potential. To further investigate the mechanism of SiHa cell apoptosis induced by ART, the ROS production, Ca^{2+} level and mitochondrial membrane potential of SiHa cells after ART treatment were detected using FCM (Figs. 3-5). The results indicated that ROS production

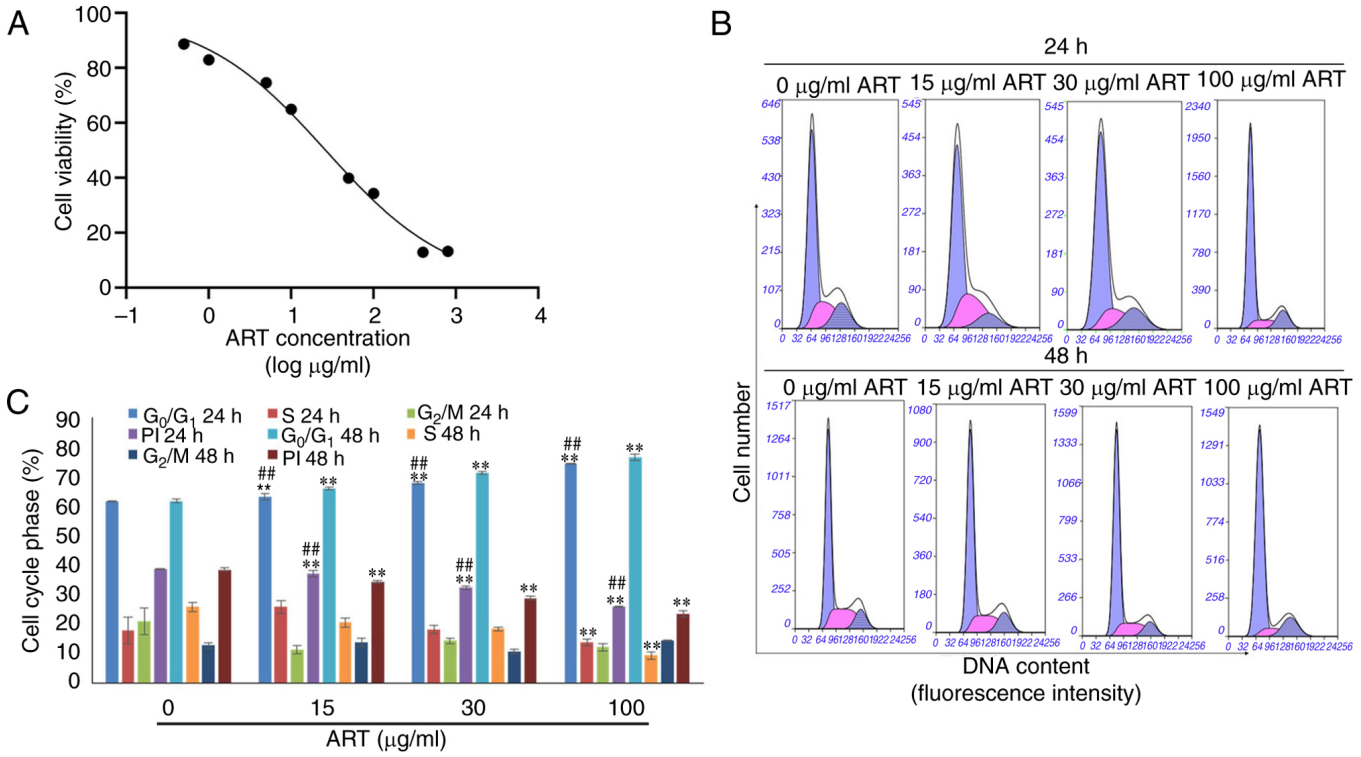

Figure 1. Inhibitory effect of ART on SiHa cells. (A) Growth curve of SiHa cells treated with ART for 24 h. A Cell Counting Kit-8 assay demonstrated that ART inhibited the proliferation of SiHa cells in a dose-dependent manner (R^2=0.9915 and half-maximal inhibitory concentration=26.32 μg/ml). (B) The cell cycle distribution of SiHa cells was detected using FCM after treatment with various concentrations of ART for 24 and 48 h. (C) FCM results demonstrated that the PI of SiHa cells was notably decreased in the ART-treated groups compared with that in the control group in a dose- and time-dependent manner. Furthermore, the proportion of cells in the G_0G_1 phase was notably increased in the ART-treated groups compared with that in the control group in a dose- and time-dependent manner. **P<0.01 vs. 0 μg/ml ART group; $^{\#\#}$P<0.01 vs. 48 h group. ART, artesunate; FCM, flow cytometry; PI, proliferation index.

in SiHa cells increased after 30 or 100 μg/ml ART treatment in a dose- and time-dependent manner (Fig. 3A). ROS production in the 30 and 100 μg/ml ART groups was significantly increased compared with that in the control group (P<0.01; Fig. 3B). Furthermore, ROS production in the 100 μg/ml ART group was significantly increased compared with that in the 15 and 30 μg/ml ART groups (P<0.01; Fig. 3B). Additionally, the Ca^{2+} concentrations in SiHa cells in the 15, 30 and 100 μg/ml ART groups were notably increased compared with that in the control group in a dose- and time-dependent manner (Fig. 4A and B). The Ca^{2+} concentration in the 100 μg/ml ART group was also significantly increased compared with that in the 15 and 30 μg/ml ART groups (P<0.01; Fig. 4B).

In addition, the mitochondrial membrane potential in the 15, 30 and 100 μg/ml ART groups was notably decreased compared with that in the control group in a dose- and time-dependent manner (Fig. 5).

Treatment with ART notably increased ROS production and Ca^{2+} and decreased the mitochondrial membrane potential, suggesting that ART triggered apoptosis in SiHa cells in a dose- and time-dependent manner accompanied by the modulation of ROS, Ca^{2+} and the mitochondrial membrane potential.

ART modulates Bcl2 family expression levels in SiHa cells. Bcl2, Bcl-xl, Mcl-1, BIM, Bok, Bax and Bak regulate cell apoptosis via pore formation in mitochondrial complexes, and the balanced expression of Bcl2, Bcl-xl, Mcl-1, BIM, Bok, Bax and Bak maintains the stability of the mitochondrial membrane. Therefore, these molecules can serve as markers for the analysis of the mechanism of action of the mitochondrial signalling pathway-induced apoptosis (31). RT-qPCR revealed notable dose- and time-dependent decreases in the expression levels of Bcl2, Bcl-xl and Mcl-1 mRNAs compared with those in the control group (Fig. 6). Furthermore, the expression levels of BIM, Bok, Bak and Bax mRNAs, which are proapoptotic gene transcripts (32), were notably upregulated in a dose- and time-dependent manner compared with that in the control group following treatment with ART for 24 and 48 h (Fig. 6). These expression profiles were in line with the increase in apoptotic activity and mitochondrial membrane modulation observed in SiHa cells after ART treatment.

Discussion

In the present study, the inhibitory effect of ART on the growth of SiHa cervical cancer cells was detected using a CCK-8 assay. ART inhibited the growth of SiHa cells in the range of 0.5-800 μg/ml ART in a concentration-dependent manner. The IC_{50} value for SiHa cells treated with ART for 24 h was 26.32 μg/ml. It was demonstrated that ART could inhibit the growth of SiHa cells, which is consistent with the findings of previous reports showing that ART inhibits the growth of tumour cells (33,34). The inhibitory effect of ART on SiHa cell growth and the underlying molecular mechanism were

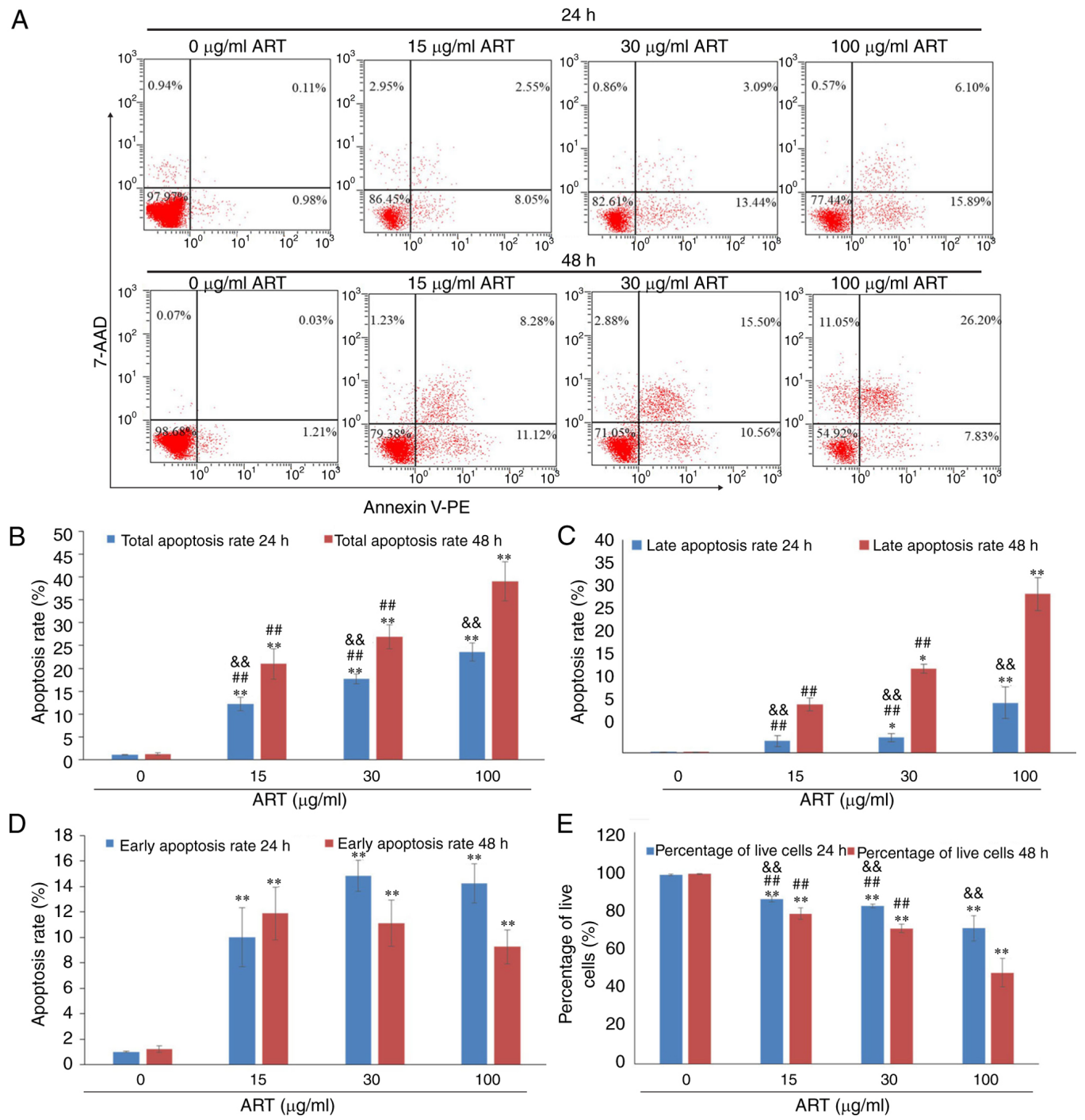

Figure 2. ART induces SiHa cell apoptosis. (A) SiHa cell apoptosis was detected using flow cytometry after treatment with various concentrations of ART for 24 and 48 h. (B) Total percentages of SiHa cells undergoing apoptosis, including early apoptotic and late apoptotic SiHa cells, were notably increased in the 15, 30 and 100 μg/ml ART groups compared with the control group in a dose- and time-dependent manner. Furthermore, the total percentage of apoptotic SiHa cells in the 100 μg/ml ART group was significantly increased compared with those in the 15 and 30 μg/ml ART groups. (C) Percentages of late apoptotic SiHa cells in the 30 and 100 μg/ml ART groups were significantly increased compared with that in the control group after treatment for 24 and 48 h in a dose-dependent manner. The percentage of late apoptotic SiHa cells in the 100 μg/ml ART group was significantly increased compared with those in the 15 and 30 μg/ml ART groups after treatment with ART for 24 and 48 h. (D) Percentages of early apoptotic SiHa cells in the 15, 30 and 100 μg/ml ART groups were significantly increased compared with that in the control group. (E) Percentages of live SiHa cells in the 15, 30 and 100 μg/ml ART groups were notably decreased compared with that in the control group in a dose- and time-dependent manner. The percentage of live SiHa cells in the 100 μg/ml ART group was significantly decreased compared with those in the 15 and 30 μg/ml ART groups after treatment with ART for 24 and 48 h. *P<0.05 and **P<0.01 vs. 0 μg/ml ART group; $^{\#\#}$P<0.01 vs. 100 μg/ml ART group; $^{\&\&}$P<0.01 vs. 48 h group. ART, artesunate.

investigated further. ART increased SiHa cell apoptosis and decreased the PI of SiHa cells.

Mitochondria are at the core of the mitochondria-mediated apoptosis pathway, and changes in the mitochondrial membrane potential are associated with cell apoptosis (35). A decrease in the mitochondrial membrane potential leads to the release of cytochrome *c*, the entry of Ca^{2+} into the cytosol and the increase in the generation of ROS, resulting in

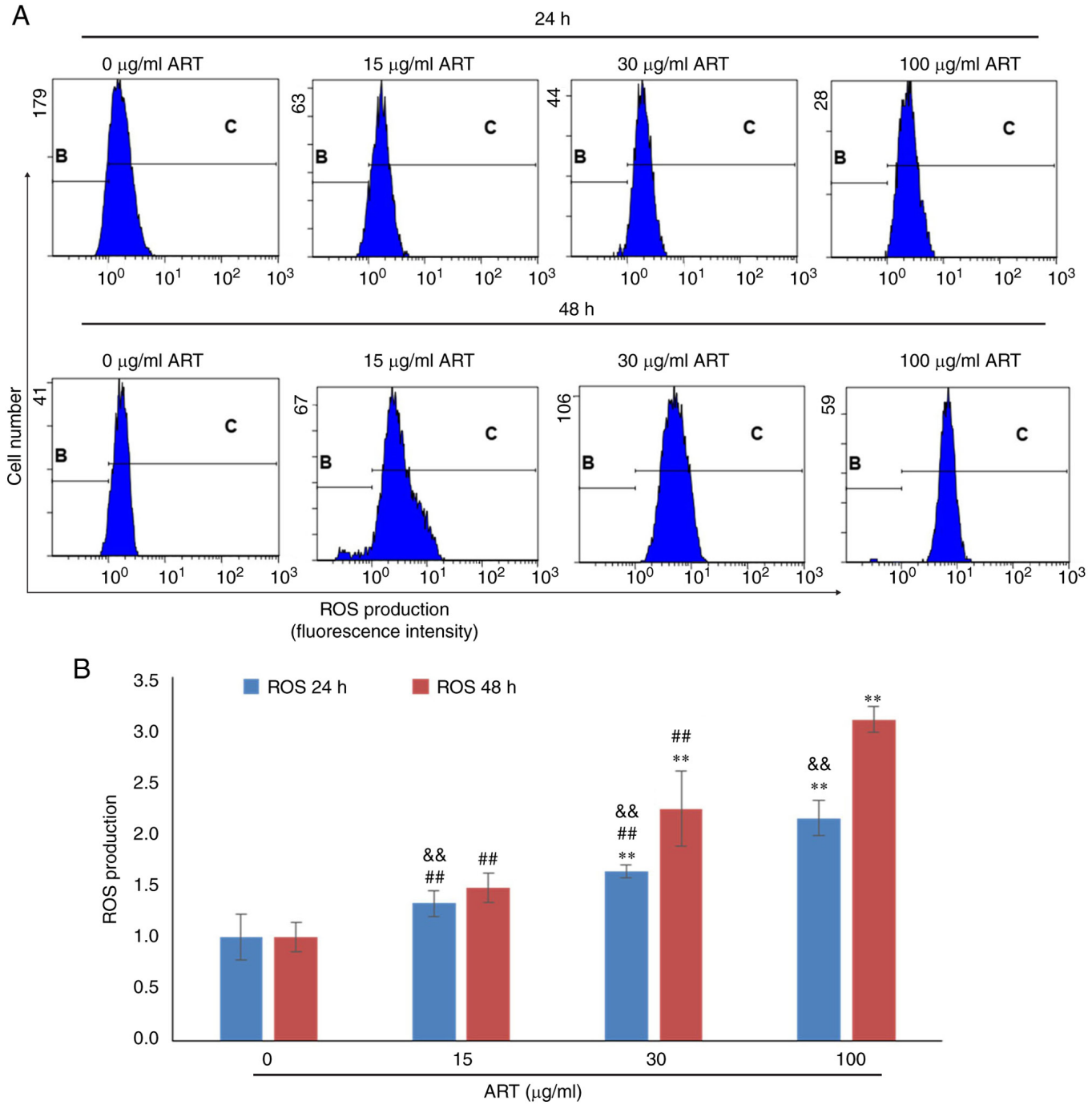

Figure 3. ART induces ROS generation in SiHa cells. (A) ROS generation in SiHa cells after treatment with ART for 24 or 48 h was detected using flow cytometry. (B) ROS generation in SiHa cells increased after ART treatment in a dose- and time-dependent manner. ROS generation in the 30 and 100 μg/ml ART groups was significantly increased compared with that in the control group. Furthermore, ROS generation in the 100 μg/ml ART group was significantly increased compared with that in the 15 and 30 μg/ml ART groups. B and C represent gates. **P<0.01 vs. 0 μg/ml ART group; $^{\#\#}$P<0.01 vs. 100 μg/ml ART group; $^{\&\&}$P<0.01 vs. 48 h group. ART, artesunate; ROS, reactive oxygen species.

irreversible apoptosis (36). Mitochondria-mediated apoptosis serves an important role in the therapeutic efficacy of new antitumour drugs, such as epigallocatechin-3-gallate and ropivacaine (22,37). In the present study, compared with those in the control group, the mitochondrial membrane potential of SiHa cells treated with 30 and 100 μg/ml ART for 24 and 48 h significantly decreased, and the production of ROS and intracellular Ca^{2+} levels significantly increased. These results are consistent with the reported mechanism of drug-induced apoptosis in tumours (38,39). Greenshields *et al* (40) reported a dose- and time-dependent inhibitory effect of ART on the growth of triple-negative MDA-MB-468 and HER2-enriched SK-BR-3 breast cancer cells. ART inhibited breast cancer cell proliferation via ROS-dependent G_2/M arrest and ROS-independent G_1 arrest. ART-treated MDA-MB-468 and SK-BR-3 cells also exhibited apoptotic cell death, which was both ROS- and iron-dependent. ART-induced oxidative stress was indicated to impair the mitochondrial outer membrane integrity and damage the cellular DNA of MDA-MB-468 and SK-BR-3 cells (27). Huang *et al* (41) reported that ART

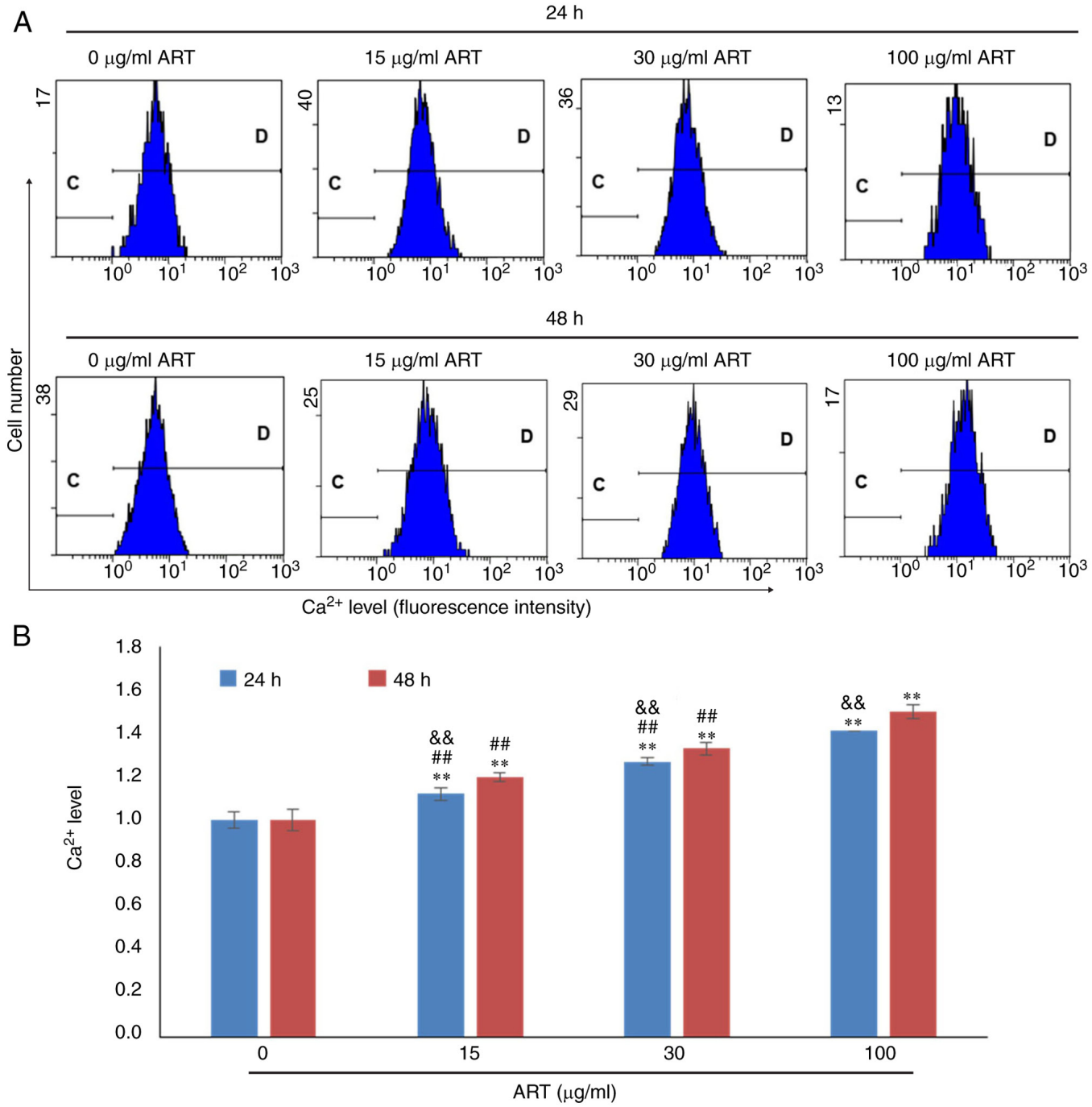

Figure 4. ART increases the Ca^{2+} concentration in SiHa cells. (A) Ca^{2+} concentrations in SiHa cells were detected using flow cytometry. (B) Ca^{2+} concentrations in SiHa cells in the 15, 30 and 100 μg/ml ART-treated groups were notably increased compared with that in the control group in a dose- and time-dependent manner. The Ca^{2+} concentration in the 100 μg/ml ART group was significantly increased compared with that in the 15 and 30 μg/ml ART groups. C and D represent gates. **P<0.01 vs. 0 μg/ml ART group; $^{\#\#}$P<0.01 vs. 100 μg/ml ART group; $^{\&\&}$P<0.01 vs. 48 h group. ART, artesunate; Ca, calcium.

serves as a senescence and autophagy inducer to exert its inhibitory effect on colorectal cancer in a ROS-dependent manner. The results of the present study suggested that ART can induce apoptosis in cervical cancer SiHa cells through a mitochondria-mediated apoptosis pathway. The molecular mechanism through which ART may regulate the mitochondrial membrane potential in SiHa cells was further investigated.

The expression profile of the Bcl2 family on the mitochondrial membrane is associated with the function of the mitochondria. A number of Bcl2 family members, including Bcl2, Bcl-xl, Mcl-1, BIM, Bax, Bok and Bak, are expressed on the outer membrane of mitochondria. In the state of increasing the Bax expression, Bax forms a heterodimer with the Bcl2 homology 3 (BH3) domain of Bcl2 and Bcl-xl (31). An increase in the expression of Bax or the expression of BIM, Bak or Bok can cause Bax to dissociate from the heterodimer and translocate from the cytosol to the mitochondrial outer membrane, possibly leading to the release of proapoptotic factors (ROS and Ca^{2+}) (32). High expression of Bcl2 in the mitochondrial outer membrane can result in binding to BIM, Bax, Bak and Bok proteins

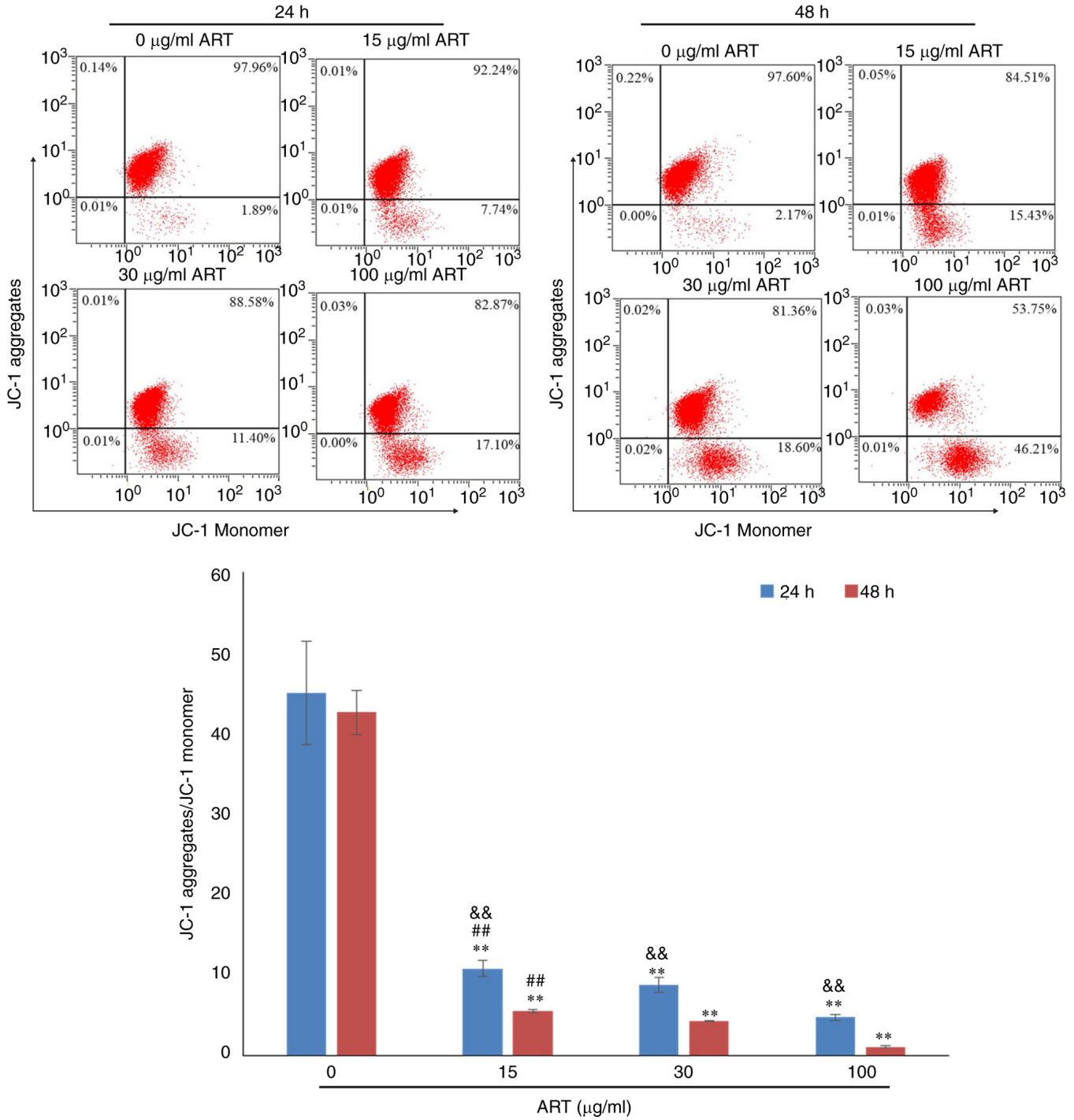

Figure 5. ART decreases the mitochondrial membrane potential of SiHa cells. After treatment with 0, 15, 30 and 100 μg/ml ART, the mitochondrial membrane potential of SiHa cells stained with JC-1 was detected using flow cytometry. The mitochondrial membrane potential of SiHa cells in the 15, 30 and 100 μg/ml ART treated groups was notably reduced compared with that in the control group in a dose- and time-dependent manner. The mitochondrial membrane potential of SiHa cells in the 100 μg/ml ART group was significantly reduced compared with that in the 15 μg/ml ART group. **P<0.01 vs. 0 μg/ml ART group; $^{\#\#}$P<0.01 vs. 100 μg/ml ART group; $^{\&\&}$P<0.01 vs. 48 h group. ART, artesunate.

to prevent their function and reduce the transmembrane flow of Ca^{2+} (42). The results of the present study revealed that the expression levels of Bcl2, Bcl-xl and Mcl-1, which inhibit apoptosis, were significantly decreased in SiHa cells treated with 15, 30 and 100 μg/ml ART for 24 and 48 h. The expression levels of the Bcl2 family members BIM, Bax, Bak and Bok were notably increased after ART treatment. Holien *et al* (43) reported that ART treatment efficiently inhibits cell growth and induces apoptosis in myeloma and diffuse large B-cell lymphoma cell lines. Apoptosis is induced concomitantly with the downregulation of Myc and antiapoptotic Bcl2 expression, as well as with the cleavage of caspase-3 (43). In this study, the role of Bcl2 family members in ART-induced apoptosis of cervical cancer SiHa cells was comprehensively studied to provide an experimental basis for the further study of the molecular mechanism through which

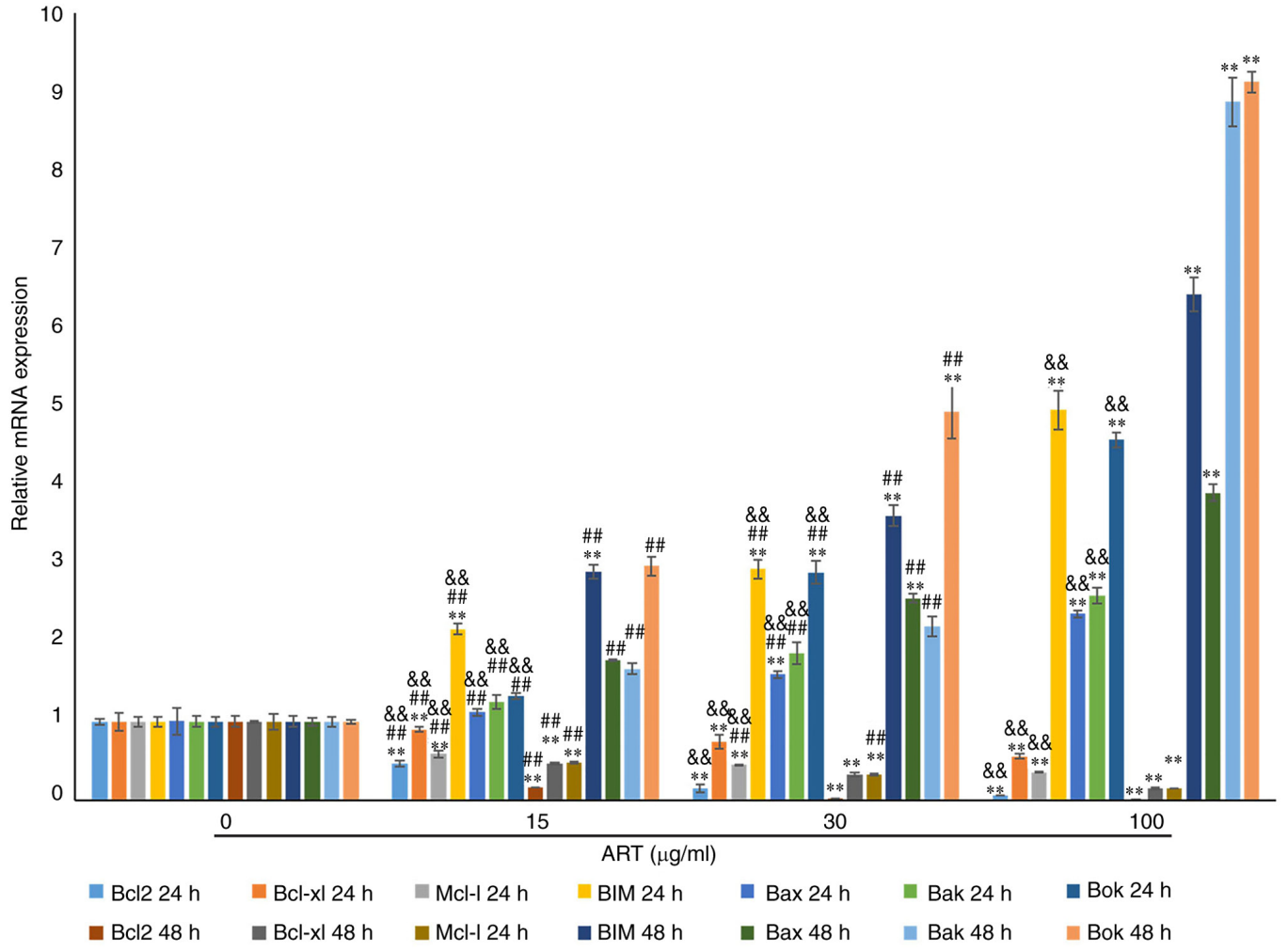

Figure 6. ART modulates the expression of the Bcl2 family in SiHa cells. RT-qPCR results showed that the mRNA expression of Bcl2, Bcl-xl and Mcl-1 in the 15, 30 and 100 μg/ml ART treated groups was notably reduced compared with that in the control group in a dose- and time-dependent manner. The mRNA expression of Bcl2, Bcl-xl and Mcl-1 in the 100 μg/ml ART group was significantly reduced compared with that in the 15 μg/ml ART group. RT-qPCR results also showed that the mRNA expression of Bax, Bak, Bok and BIM in the 15, 30 and 100 μg/ml ART treated groups was notably increased compared with that in the control group in a dose- and time-dependent manner. The mRNA expression of Bax, Bak, Bok and BIM in the 100 μg/ml ART group was significantly increased compared with that in the 15 and 30 μg/ml ART groups (P<0.01). **P<0.01 vs. 0 μg/ml ART group; $^{\#\#}$P<0.01 vs. 100 μg/ml ART group; $^{\&\&}$P<0.01 vs. 48 h group. ART, artesunate; RT-qPCR, reverse transcription-quantitative PCR.

ART regulates the mitochondrial membrane potential of SiHa cells. Furthermore, in the present study, the association between the expression of the multimolecular Bcl2 family and mitochondrial apoptosis was investigated. To the best of our knowledge, the molecular mechanism via which ART regulates the Bcl2 family molecules to induce apoptosis by modulating the mitochondrial membrane potential has not been reported in the literature. However, the lack of western blotting experiments was a limitation of the present study that should be conducted in future studies.

At present, a number of studies on the antitumour effect of ART have been reported (41,44,45). In the present study, ART-induced apoptosis in cervical cancer SiHa cells through the induction of the mitochondria-mediated apoptosis pathway was investigated. Additionally, the molecular mechanism through which ART may regulate the mitochondrial membrane potential was also explored. The results of the present study revealed that ART had an anti-growth effect on SiHa cervical cancer cells, and the mechanism was associated with the induction of SiHa cell apoptosis and inhibition of cell proliferation. The mechanism of apoptosis induction is associated with the regulation of the expression levels of the Bcl2 family members Bcl2, Bcl-xl, Mcl-1, BIM, Bax, Bak and Bok, which mediate the mitochondrial apoptosis pathway (31,32,42). The present study provides an experimental basis for the clinical application of ART as an anticancer drug. Other potential anticancer mechanisms of ART, such as the molecular mechanism associated with inhibiting cell proliferation and inducing cell apoptosis, will be investigated in future studies. In further experiments, the toxic effects of ART on cervical cancer cells using non-cancer cervical cells and positive drug groups will also be investigated.

In conclusion, ART had an antiproliferative effect on SiHa cervical cancer cells, and the mechanism was associated with the induction of SiHa cell apoptosis and inhibition of cell proliferation. The mechanism of apoptosis induction may involve the regulation of the Bcl2 family members Bcl2, Bcl-xl, Mcl-1, BIM, Bax, Bak and Bok, which mediate the

mitochondrial apoptosis pathway. The molecular mechanism of ART-induced SiHa cell apoptosis should be studied further, and the molecular mechanism through which ART inhibits cell proliferation should also be investigated in future experiments.

Acknowledgements

Not applicable.

Funding

This study was supported by the Key Medical Science Project of Hebei Province (grant no. 20211027).

Availability of data and materials

The data generated in the present study may be requested from the corresponding author.

Authors' contributions

QZ performed the experiments and wrote the manuscript. XL and CH performed the experiments and the statistical analysis. RZ and JW performed the experiments. LL designed and performed the experiments, and revised the manuscript. All authors read and approved the final manuscript. QZ and LL confirm the authenticity of all the raw data.

Ethics approval and consent to participate

Not applicable.

Patient consent for publication

Not applicable.

Competing interests

The authors declare that they have no competing interests.

References

1. Sung H, Ferlay J, Siegel RL, Laversanne M, Soerjomataram I, Jemal A and Bray F: Global Cancer statistics 2020: GLOBOCAN estimates of incidence and mortality worldwide for 36 cancers in 185 countries. CA Cancer J Clin 71: 209-249, 2021.
2. Gu XY, Zheng RS, Sun KX, Zhang SW, Zeng HM, Zou XN, Chen WQ and He J: Incidence and mortality of cervical cancer in China, 2014. Zhonghua Zhong Liu Za Zhi 40: 241-246, 2018 (In Chinese).
3. Kaidar-Person O, Bortnyak-Abdah R, Amit A, Berniger A, Ben-Yosef R and Kuten A: Current principles for radiotherapy in cervical cancer. Med Oncol 29: 2919-2922, 2012.
4. Sharma S, Deep A and Sharma AK: Current treatment for cervical cancer: An update. Anticancer Agents Med Chem 20: 1768-1779, 2020.
5. Diaz-Padilla I, Monk BJ, Mackay HJ and Oaknin A: Treatment of metastatic cervical cancer: Future directions involving targeted agents. Crit Rev Oncol Hematol 85: 303-314, 2013.
6. Lefèvre A and Léonard P: Artesunate and severe malaria in paediatrics. Rev Med Liege 74: 503-507, 2019.
7. Abanyie F, Acharya SD, Leavy I, Bowe M and Tan KR: Safety and effectiveness of intravenous artesunate for treatment of severe malaria in the united States-April 2019 through december 2020. Clin Infect Dis 73: 1965-1972, 2021.
8. Roussel C, Ndour PA, Kendjo E, Larréché S, Taieb A, Henry B, Lebrun-Vignes B, Chambrion C, Argy N, Houzé S, *et al*: Intravenous artesunate for the treatment of severe imported malaria: Implementation, efficacy, and safety in 1391 patients. Clin Infect Dis 73: 1795-1804, 2021.
9. Tsuda K, Miyamoto L, Hamano S, Morimoto Y, Kangawa Y, Fukue C, Kagawa Y, Horinouchi Y, Xu W, Ikeda Y, *et al*: Mechanisms of the pH- and Oxygen-dependent oxidation activities of artesunate. Biol Pharmaceutical Bull 41: 555-563, 2018.
10. Li T, Chen H, Liu XG, Zhou YX and Bai SF: Immunoregulatory effect of artesunate on allergic contact dermatitis and its mechanism. Yao Xue Xue Bao 47: 884-889, 2012.
11. Meng QF, Zhang XX, Zhang Z, Chen W, Li XL, Wang YJ, Li FF and Li YB: Therapeutic potential of artesunate in experimental autoimmune myasthenia gravis by upregulated T regulatory cells and regulation of Th1/Th2 cytokines. Pharmazie 73: 526-532, 2018.
12. Wang N, Zeng GZ, Yin JL and Bian ZX: Artesunate activates the ATF4-CHOP-CHAC1 pathway and affects ferroptosis in Burkitt's Lymphoma. Biochem Biophys Res Commun 519: 533-539, 2019.
13. Jiang F, Zhou JY, Zhang D, Liu MH and Chen YG: Artesunate induces apoptosis and autophagy in HCT116 colon cancer cells, and autophagy inhibition enhances the artesunate-induced apoptosis. Int J Mol Med 42: 1295-1304, 2018.
14. Zhao F, Vakhrusheva O, Markowitsch SD, Slade KS, Tsaur I, Cinatl J Jr, Michaelis M, Efferth T, Haferkamp A and Juengel E: Artesunate impairs growth in cisplatin-resistant bladder cancer cells by cell cycle arrest, apoptosis and autophagy induction. Cells 9: 2643, 2020.
15. Chen S, Gan S, Han L, Li X, Xie X, Zou D and Sun H: Artesunate induces apoptosis and inhibits the proliferation, stemness, and tumorigenesis of leukemia. Ann Transl Med 8: 767, 2020.
16. Våtsveen TK, Myhre MR, Steen CB, Wälchli S, Lingjærde OC, Bai B, Dillard P, Theodossiou TA, Holien T, Sundan A, *et al*: Artesunate shows potent anti-tumor activity in B-cell lymphoma. J Hematol Oncol 11: 23, 2018.
17. Yin X, Liu Y, Qin J, Wu Y, Huang J, Zhao Q, Dang T, Tian Y, Yu P and Huang X: Artesunate suppresses the proliferation and development of estrogen receptor-α-Positive endometrial cancer in HAND2-Dependent pathway. Front Cell Dev Biol 8: 606969, 2020.
18. Mancuso RI, Foglio MA and Olalla Saad ST: Artemisinin-type drugs for the treatment of hematological malignancies. Cancer Chemother Pharmacol 87: 1-22, 2021.
19. Liu L, Zuo LF, Zuo J and Wang J: Artesunate induces apoptosis and inhibits growth of Eca109 and Ec9706 human esophageal cancer cell lines *in vitro* and *in vivo*. Mol Med Rep 12: 1465-1472, 2015.
20. Wang L, Liu L, Wang J and Chen Y: Inhibitory effect of artesunate on growth and apoptosis of gastric cancer cells. Arch Med Res 48: 623-630, 2017.
21. Saeed MEM, Cives-Losada C and Efferth T: Biomarker expression profiling in cervix carcinoma biopsies unravels WT1 as a target of artesunate. Cancer Genomics Proteomics 19: 727-739, 2022.
22. Liu L, Ju Y, Wang J and Zhou R: Epigallocatechin-3-gallate promotes apoptosis and reversal of multidrug resistance in esophageal cancer cells. Pathol Res Pract 213: 1242-1250, 2017.
23. Kriváková P, Cervinková Z, Lotková H, Kucera O and Rousar T: Mitochondria and their role in cell metabolism. Acta Medica (Hradec Kralove) Suppl 48: 57-67, 2005 (In Czech).
24. Estaquier J, Vallette F, Vayssiere JL and Mignotte B: The mitochondrial pathways of apoptosis. Adv Exp Med Biol 942: 157-183, 2012.
25. Lopez J and Tait SW: Mitochondrial apoptosis: Killing cancer using the enemy within. Br J Cancer 112: 957-962, 2015.
26. Jeong SY and Seol DW: The role of mitochondria in apoptosis. BMB Rep 41: 11-22, 2008.
27. Kaloni D, Diepstraten ST, Strasser A and Kelly GL: BCL-2 protein family: Attractive targets for cancer therapy. Apoptosis 28: 20-38, 2023.
28. Kashyap D, Garg VK and Goel N: Intrinsic and extrinsic pathways of apoptosis: Role in cancer development and prognosis. Adv Protein Chem Struct Biol 125: 73-120, 2021.
29. Liu Y, Ju Y, Liu J, Chen Y, Huo X and Liu L: Inhibition of proliferation and migration and induction of apoptosis in glioma cells by silencing TLR4 expression levels via RNA interference. Oncol Lett 21: 13, 2021.

30. Livak KJ and Schmittgen TD: Analysis of relative gene expression data using real-time quantitative PCR and the 2(-Delta Delta C(T)) method. Methods 25: 402-408, 2001.
31. Warren CFA, Wong-Brown MW and Bowden NA: BCL-2 family isoforms in apoptosis and cancer. Cell Death Dis 10: 177, 2019.
32. Hafezi S and Rahmani M: Targeting BCL-2 in cancer: Advances, challenges, and perspectives. Cancers (Basel) 13: 1292, 2021.
33. Wen L, Lv G, Zhao J, Lu S, Gong Y, Li Y, Zheng H, Chen B, Gao H, Tian C and Wang J: In vitro and in vivo effects of artesunate on echinococcus granulosus protoscoleces and metacestodes. Drug Des Devel Ther 14: 4685-4694, 2020.
34. Li Q, Ni W, Deng Z, Liu M, She L and Xie Q: Targeting nasopharyngeal carcinoma by artesunate through inhibiting Akt/mTOR and inducing oxidative stress. Fundam Clin Pharmacol 31: 301-310, 2017.
35. Abate M, Festa A, Falco M, Lombardi A, Luce A, Grimaldi A, Zappavigna S, Sperlongano P, Irace C, Caraglia M and Misso G: Mitochondria as playmakers of apoptosis, autophagy and senescence. Semin Cell Dev Bio 98: 139-153, 2020.
36. Li J, Cui J, Li Z, Fu X, Li J, Li H, Wang S and Zhang M: ORP8 induces apoptosis by releasing cytochrome c from mitochondria in non-small cell lung cancer. Oncol Rep 43: 1516-1524, 2020.
37. Wang W, Zhu M, Xu Z, Li W, Dong X, Chen Y, Lin B and Li M: Ropivacaine promotes apoptosis of hepatocellular carcinoma cells through damaging mitochondria and activating caspase-3 activity. Biol Res 52: 36, 2019.
38. Zhou X, Chen Y, Wang F, Wu H, Zhang Y, Liu J, Cai Y, Huang S, He N, Hu Z and Jin X: Artesunate induces autophagy dependent apoptosis through upregulating ROS and activating AMPK-mTOR-ULK1 axis in human bladder cancer cells. Chem Biol Interact 331: 109273, 2020.
39. Ji P, Huang H, Yuan S, Wang L, Wang S, Chen Y, Feng N, Veroniaina H, Wu Z, Wu Z and Qi X: ROS-mediated apoptosis and anticancer effect achieved by artesunate and auxiliary fe(II) released from ferriferous Oxide-Containing recombinant apoferritin. Adv Healthc Mater 8: e1900911, 2019.
40. Greenshields AL, Fernando W and Hoskin DW: The anti-malarial drug artesunate causes cell cycle arrest and apoptosis of triple-negative MDA-MB-468 and HER2-enriched SK-BR-3 breast cancer cells. Exp Mol Pathol 107: 10-22, 2019.
41. Huang Z, Gan S, Zhuang X, Chen Y, Lu L, Wang Y, Qi X, Feng Q, Huang Q, Du B, *et al*: Artesunate Inhibits the cell growth in colorectal cancer by promoting ROS-Dependent cell senescence and autophagy. Cells 11: 2472, 2022.
42. Qian S, Wei Z, Yang W, Huang J, Yang Y and Wang J: The role of BCL-2 family proteins in regulating apoptosis and cancer therapy. Front Oncol 12: 985363, 2022.
43. Holien T, Olsen OE, Misund K, Hella H, Waage A, Rø TB and Sundan A: Lymphoma and myeloma cells are highly sensitive to growth arrest and apoptosis induced by artesunate. Eur J Haematol 91: 339-346, 2013.
44. Cao D, Chen D, Xia JN, Wang WY, Zhu GY, Chen LW, Zhang C, Tan B, Li H and Li YW: Artesunate promoted anti-tumor immunity and overcame EGFR-TKI resistance in non-small-cell lung cancer by enhancing oncogenic TAZ degradation. Biomed Pharmacothe 155: 113705, 2022.
45. Li ZJ, Dai HQ, Huang XW, Feng J, Deng JH, Wang ZX, Yang XM, Liu YJ, Wu Y, Chen PH, *et al*: Artesunate synergizes with sorafenib to induce ferroptosis in hepatocellular carcinoma. Acta Pharmacol Sin 42: 301-310, 2021.